REVISTA MATÉRIA V.24 N.02
ISSN 1517-7076 articles e-12379, 2019

# Characterization of new selective coatings, made of granite and chrome, for solar collectors

Felipe Alves Albuquerque Araújo[1], Francisco Nivaldo Aguiar Freire[2], Diego Caitano Pinho[2], Kaio Hemerson Dutra[2], Paulo Alexandre Costa Rocha[2], Maria Eugênia Vieira da Silva[2]

[1] Laboratório em Filmes Finos em Energias Renováveis - LAFFER, PPGECM/UFC ,CEP: 60.440-554, Fortaleza, Ceará, Brasil.
[2] Universidade Federal do Ceará - UFC, Avenida Mister Hull, s/n, Campus do Pici, Fortaleza, Ceará, Brasil.
e-mail: fel.albuquerque@hotmail.com, nivaldo@ufc.br, diegopynho@gmail.com, kaiohdutra@hotmail.com, paulo.rocha@ufc.br, eugenia@ufc.br

## ABSTRACT

The depletion of fossil fuel reserves and climate change caused by atmospheric pollution has led the human being to seek alternatives that are less damaging to the environment. The concern and the awareness of the population open space for the study of renewable energies to be deepened, among them the best use of solar energy.

The use of alternative materials to replace selective surfaces is a natural trend, since improvements in surface efficiency are usually sought while attempting to reduce costs. Composite substances are already used to obtain some selective surfaces, and, as a result, the search for better processes awakens research on more appropriate and lower cost materials, which represents a great scientific potential in the evolution of these technologies.

Thus, the present work consisted in obtaining and studying selective surfaces for applications in low-cost flat plate solar collectors, using residues from the granite industry. Five different surfaces were studied, varying the weight percentage: 100% granite powder, 75% granite powder + 25% chromium oxide, 50% granite powder + 50% chromium oxide, 25% granite powder + 75% chromium oxide and 100% chromium oxide.

For the tests, an experimental wooden stand was built, and it was possible to simulate the conditions of a flat plate solar collector. To characterize the surfaces, scanning electron microscope (SEM) techniques, infrared analysis, X-ray diffraction and UV-VIS absorbance determination, as well as graphs with surface temperatures and with radiation, during the tests in the sun, were used.

The surfaces` efficiency was determined by the ratio of the absorptivity by the emissivity, as well as the trademark **MR**TiNOX, a commercial selective surface applied on copper substrate. For this, an efficiency of 23.56 was obtained, while for the 50% granite and 50% chromium surfaces the value of 23.27 (closest to the trade mark) was calculated. Therefore, replacing the traditional components of selective surfaces with granite proved to be a satisfactory solution, contributing to the reduction of costs with work involving solar energy.

**Keywords:** solar energy; selective surface; granite; chromium oxide; efficiency.

## 1. INTRODUCTION

The Sun is the great renewable energy source of the planet. It can serve as both a source of light and a source of heat, making it one of the most promising energy alternatives to overcome the hardships of the new millennium.

Solar energy is, by excellence, the most ecologically correct. It is abundant, renewable and clean. Working as a huge fusion reactor, the Sun radiates a high energy potential every day, incomparable to any other energy system [1].

Nowadays, the human being has been looking for clean energy sources because, with the changes in climatic conditions caused by atmospheric pollution, in addition to the depletion of fossil fuel reserves, there

Autor Responsável: Felipe Alves Albuquerque Araújo Data de envio:06/092018 Data de aceite: 21/01/2019

10.1590/S1517-707620190002.0694

is a greater awareness and concern of the population regarding the use of renewable energies.

In Brazil, in 2014, 39.4% of all energy produced came from renewable sources, and the energy generated in hydroelectric plants represented 29.2%, which is reflected in 65.2% of the electric energy produced. Wind and solar energy make up only 2% of the electricity produced in the country and does not have significant representation in the total percentage of energy (which includes electric, thermal and chemical energy). With regard to fossil fuels, these are responsible for almost 60% of all energy generated [2].

Considering that the solar incidence on the continental masses, in one year, corresponds to $1.74 \times 10^{11}$ GWh, and that the annual energy consumption corresponds to $1.5 \times 10^{8}$ GWh, it is verified that the available solar energy represents more than 1,000 times the energy consumption of mankind. Therefore, less than 1% of the total energy incident on the continental masses would supply the world's energy demand. If the total area of the Earth was taken into account, this availability would rise to $1.02 \times 10^{13}$ GWh [3].

Solar energy can be used in the form of photovoltaic energy and solar thermal energy, which are non-polluting energy sources, unlike the vast majority of energy sources that pollute and harm the planet [4].

One of the ways to take advantage of solar thermal energy is through solar collectors, which basically consist of surfaces that absorb the thermal energy from the sun. Initially, it was observed that black surfaces were able to absorb the thermal energy of the sun, and therefore the first proposed surfaces for solar thermal collectors were simply painted black. As the study of this type of collector involves heat transfer, there are so-called thermal losses, which must be considered in energy balances. They occur, basically, due to reflection and emission, which are linked to two thermal properties of the material, the reflectivity and the emissivity.

The surface`s coating of the solar radiation absorber plates has a fundamental function in the absorption and reflection of this radiation, as well as in the emission of thermal radiation, directly influencing the efficiency of the collectors, as well as their cost-benefit relation. As absorptivity, reflectivity and emissivity are intrinsic characteristics of the materials, it is necessary to obtain those that are capable of absorbing the maximum of solar radiation, reflecting as little of this radiation as possible and also emitting as little as possible for the external environment. Surfaces containing these characteristics are called selective surfaces. According to [5], selective surfaces can be classified into six major groups: intrinsic; semiconductor-metal pairs; multilayer absorbers; coatings with composite materials; rough surfaces; transparent coatings on absorbent substrates.

Selective surfaces on copper and on glass, using Cr-$Cr_2O_3$ and Mo-$Al_2O_3$ cermet, by means of magnetron sputtering deposition, were produced by [6] in 2001. By varying the oxygen flow during the deposition procedure, there were obtained multilayer surfaces with Cr-$Cr_2O_3$ cermet, which contributed to the improvement of optical performance. With this deposition technique, absorbance of 0.94 and emitance of 0.04 were verified using Cr-$Cr_2O_3$ on copper substrate. With Mo-$Al_2O_3$, although the absorbance was the same as 0.94, the emitance value increased to 0.09.

In 2005, [7] carried out experimental studies on silicon-carbon dissolved in aqueous media and deposited by spin-coating on a glass substrate of different thicknesses, and then passed through a heat treatment. The objective was to evaluate the emissivity and the absorbance of the surfaces, and the best results were found for films with a thickness of 1000nm, which presented absorbance of 0.94 and emissivity of 0.15.

In 2007, [8] worked with TiAlN / TiAlON / Si3N4 in the production of selective surfaces, having the first two layers absorbing characteristics, and the third acting as an anti-reflective layer. Through the deposition technique known as reactive magnetron sputtering DC, the multilayer surface was applied to four different substrates: stainless steel, nickel, copper and **MR**Nimonic. Among the different applications of multilayers, the one that gave the best results reached, at a temperature of 82ºC, absorbance of 0.958 and emitance of 0.07, for deposition on copper substrates.

In 2010, the Federal Government of Brazil launched the My Home My Life with Solar Heating Program, through which several popular homes were financed by the Federal Government and delivered with a water heating system using solar energy. The main goals of the program were to avoid the use of electric showers (very common in the South and Southeast regions of Brazil) and to allow the use of hot water to better sanitize the dishes, which reduces the risk of disease contraction [9].

In 2013, [10] worked with CrMoN (H) / CrMoN (L) / CrON in the production of selective surfaces, making use of magnetron sputtering deposition DC reactive technique. For work at low temperatures, the surfaces applied on aluminum substrate were used, and at medium temperatures the stainless steel substrate

was chosen. At a temperature of 82 ° C, the CrMoN / CrON layers reached absorbance values of 0.90 and emissance of 0.08, when applied on aluminum substrate. On the other hand, with average temperatures, absorbance values of 0.92 and emitance of 0.13 were obtained with the multilayer surfaces applied on stainless steel.

The objectives are synthesize and study selective surfaces for applications in low-cost flat plate solar collectors using chromium oxide and waste from the granite industry. It is intended to achieve a similar or even higher efficiency than the selective surfaces already on the market, thus making the process of manufacturing solar collectors more efficient, since reducing costs and manufacturing time is directly linked to the current import requirement of these surfaces.

## 2. MATERIALS AND METHODS

In this section, the procedures performed for synthesizing and characterizing the selective surfaces are presented, as well as for the construction of a new test bench in order to evaluate and compare the new surfaces with the commercial one (**MR**TiNOX).

### 2.1 Surfaces preparation

The granite used in the present work is the green-ubatuba, as it is known commercially. To obtain the compound to be deposited on the substrate, firstly occurred the maceration of the granite. The procedure consisted in first breaking an entire block into smaller pieces with the use of a sledgehammer, obtaining granite grains. These were powdered through the use of a planetary mill, by inserting in the tech pots 97g of zirconium balls for every 10g of granite grains. The milling occurred for one hour, with rotation of 360rpm.

With the granite powder, it was necessary to perform a separation according to the granulometry, since the diameters were not homogeneous. For this, sieves with different MESH numbers were arranged, collecting the contents retained in the one of number MESH 200, that has aperture of 0.075mm.

The composites were produced with the use of granite powder and chromium oxide, being combined in the following proportions: 25% -75%, 50% -50% and 75% -25%. Two other surfaces were also synthesized: one with 100% granite and the other with 100% chromium.

As the samples produced were in the form of powder, the use of binders was necessary to make adhesion to the base material, transforming them into elements with viscous characteristics and adhering to metallic surfaces. Two types of different binders, **MR**Araldite type A and type B, were tested by [11] and [12]. In this work, another binder, brand **MR**Nauticola B, was chosen to perform the adhesion to the copper plates (substrate). To complete the deposited compound, the amount of 3%, by weight of the total amount of the samples, of B2O3 / Bi2O3 flux (a mixture of boron-bismuth in a 1: 1 molar ratio) was added. The compositions of each selective surface produced are set forth in Table 1.

**Table 1**: Composition of selective surfaces obtained.

| COMPONENTS | SURFACE 1 | SURFACE 2 | SURFACE 3 | SURFACE 4 | SURFACE 5 |
|---|---|---|---|---|---|
| Granite powder [%] | 62,0 | - | 20,7 | 31,0 | 41,3 |
| Chromium oxide [%] | - | 62,0 | 41,3 | 31,0 | 21,7 |
| **MR**Nauticola B [%] | 35,0 | 35,0 | 35,0 | 35,0 | 35,0 |
| Flux [%] | 3,0 | 3,0 | 3,0 | 3,0 | 3,0 |
| Total mass [g] | 1,6 | 1,6 | 1,6 | 1,6 | 1,6 |

After obtaining the compounds, the deposition was made on a copper substrate (4cm x 2cm plate, approximately 0.3mm thick), by means of the process known as “screen printing”, in which a spatula is used to perform the scattering of those on this. Subsequently, the surfaces were heat treated (sintering) in a resistive kiln, following the parameters shown in Figure 1, so that the binder evaporated and, thus, the sintering process of the deposited compounds was completed. The heating rate was 0.5ºC / min, and the cooling of the copper plates occurred inside the kiln.


**Figure 1:** Sintering parameters.

### 2.2 Test bench

To perform the field tests, an experimental bench with a box - like structure was constructed from 2.5cm thick muiracatiara wood with a colorless, tempered, 1m x 12.6cm and thickness of 4mm **MR**Vivix float type glass cover. The workbench was divided into nine equal compartments, being covered in the lower part by rectangular pieces of glass wool, 11.5cm x 8.5cm and a thickness of 5cm. The copper plates, with the selective surfaces deposited, were placed in each of these compartments, above the glass wool insulation, for testing in the sun. In Figure 2, there is the bench on one of the days of tests performed with exposure to solar radiation.

**Figure 2:** Experimental bench for tests in the sun.

The bench was also composed of k-type thermocouples, for measuring the temperatures of the selective surfaces, the environment, the glass and the insulation, of an **MR**Eppley Horizontal Piranometer,

for the measurement of solar radiation, and of a datalogger, in order to register the obtained values.

### 2.3 Performed tests

To characterize and verify the performance of the new selective surfaces obtained, the following tests were performed:

1. Verification of the morphological structure and chemical composition resulting from the synthesization of the material by means of EDX micro scanning electron microscopy (SEM), at the Analytical Center of the Federal University of Ceará (UFC);

2. Infrared analysis, with KBr inserts, in the Shimadzu apparatus, IRTracer-100 model, in the range of 400 to 4000cm$^{-1}$, in order to determine if any composites were formed after the surfaces preparation in the resistive kiln;

3. X-ray diffraction data refinement analysis for the structural characterization of the composites obtained in the UFC X-ray Diffraction Laboratory;

4. Absorbance graphs, in the range of 185nm to 1000nm, obtained by analyzing the selective surfaces deposited in glass on Shimadzu's Uv-vis Spectrophotometer, Uv-2600;

5. Comparison between the performances of the surfaces, by means of tests carried out on the manufactured bench, in real ambient conditions, with temperature measurements and with calculations of absorbance and emitance.

## 3. RESULTS

This section covers all the results obtained, being: average temperature and radiation graphs for tests in the sun, on March 12, 13, 14 and 17, 2018, from 10:30 a.m. to 4:30 p.m.; absorbance graphs of the selective surfaces produced, mainly observing the visible light range (400nm to 750nm); graph of infrared analysis, comparing the peaks found; diffractogram of a sample with 50% granite and 50% chromium, with the respective components found; morphological characteristics and composition of selective surfaces produced and commercial, from images obtained in the SEM.

### 3.1 Field tests

Some tests in the sun were performed during the month of March 2018. Those that occurred in the presence of many clouds or even rain were excluded, taking into account only the data obtained on days 12, 13, 14 and 17. Temperatures of six selective surfaces were saved every two minutes: granite; granite 75% - chrome 25%; 50% granite - 50% chromium; 25% granite - 75% chrome; chrome; **MR**TiNOX. Also were measured the temperatures of the glass cover, the insulation and the environment. The temperature averages, when the system reached the permanent regime, measured from 11h to 12:30h, are in Table 2.

**Table 2:** Average temperatures for steady state operation.

| MEASURED ELEMENTS | AVERAGE TEMPERATURE (ºC) |
|---|---|
| Surface 100% granite | 87,3 |
| Surface granite 75% - chrome 25% | 86,2 |
| Surface granite 50% - chrome 50% | 87,4 |
| Surface granite 25% - chrome 75% | 88,5 |
| Surface 100% chrome | 90,5 |
| **MR**TiNOX | 92,7 |
| Glass cover | 67,8 |
| Insulation | 37,1 |
| Environment | 34,0 |

The average radiation for the four days, in the steady state period (11:00 a.m. to 12:30 p.m.), was 938.4 W/m². The graph for the entire operating time range, from 10:30 a.m. to 4:30 p.m., with average temperatures and radiation, is shown in Figure 3.

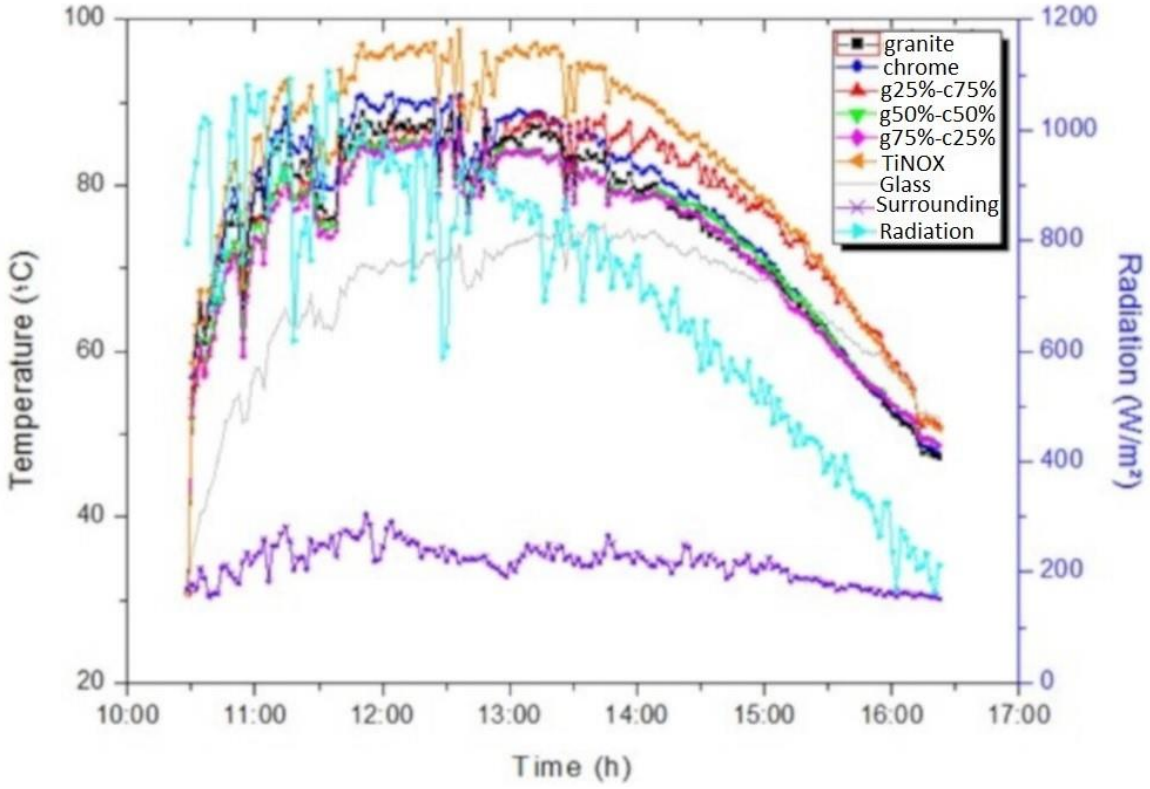


**Figure 3:** Comparison between average temperatures of selective surfaces.

### 3.2 Absorbance graphs of surfaces

One of the most important factors to consider in choosing a selective surface is the absorbance of each of them. Using Shimadzu's Uv-vis Spectrophotometer, Uv-2600, it was possible to plot the graphs in the wavelength range from 185nm to 1000nm, as shown in Figure 4.

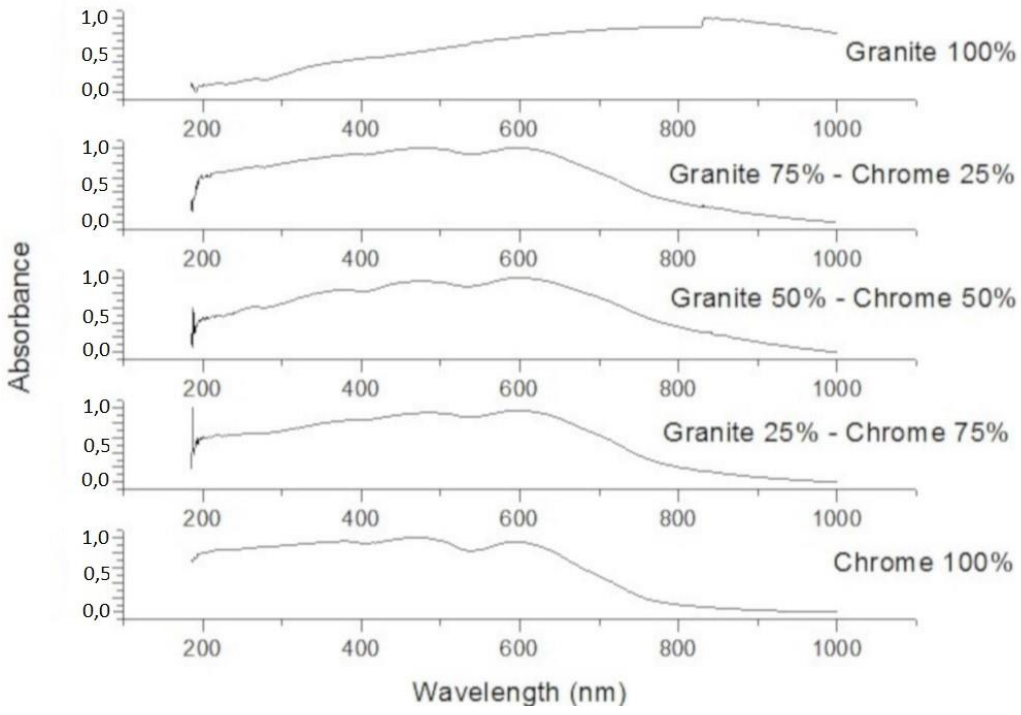


**Figure 4:** Absorbance graphs of selective surfaces produced.

It is observed that, in surfaces containing chrome, the absorbance in the visible light range (400nm to 750nm) has a maximum value, which is a positive factor for better solar energy capture. It is shown in the graph of the surface with only granite a tendency of growth of the absorption in the range of 185nm to approximately 830nm. From there, the curve of the graph begins to show a decay.

### 3.3 Analyzes in the SEM

Electron microscopes are those that work by means of a beam of electrons, having capacity of magnification superior to the light´s microscopes. They are basically divided into two main types: Electronic Transmission Electron Microscope (MET) and Scanning Electron Microscope (SEM).

According to [13], MET is more recommended in the study of finer details of a cellular structure or of a molecular organization of viruses or subcellular constituents. This type of microscope has the disadvantages of being relatively complex, the specimens must be quite thin and, working with structures in three dimensions, the necessary information are more difficult to obtain. The SEM is the most used when studying the topography of surfaces of solid objects, although it does not provide (or provides very little) information about internal structures.

The SEM is a device with high resolution capability, through which it is possible to obtain images with great clarity with, for example, 10,000 times of magnification. The use of SEM with microprobe EDX (Energy Dispersive X-ray) is very useful in the investigation of microstructures, allowing elemental chemical analysis [14].

The micrographs, obtained through SEM, revealed the disposition of selective surfaces on the copper substrate. In Figures 5 to 8, morphological characteristics of the surfaces produced, according to the data of Table 1, are revealed.

In Figure 5, the chromium oxide particles appear to be leaving the composition of the selective surface, and it is possible to observe a dispersion of their grains. There is little unfilled space, being the copper substrate almost completely occupied. A difference in grain size can also be seen in the same figure.

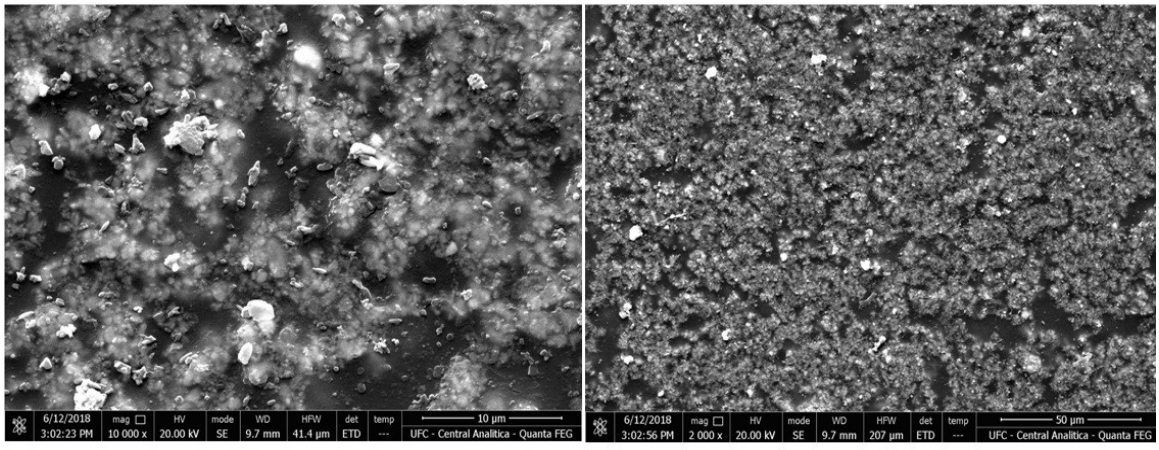


(a) (b)

**Figure 5:** Micrograph of the selective surface sample of 100% chromium oxide, with magnification factor of: (a) 10000x and (b) 2000x.

It is shown in Figure 6 the surface of 50% chromium oxide - 50% granite powder, in which it is possible to verify exposed grains containing chrome, carbon, oxygen, silicon, iron and aluminum, contrasting with a large area of unfilled copper substrate.

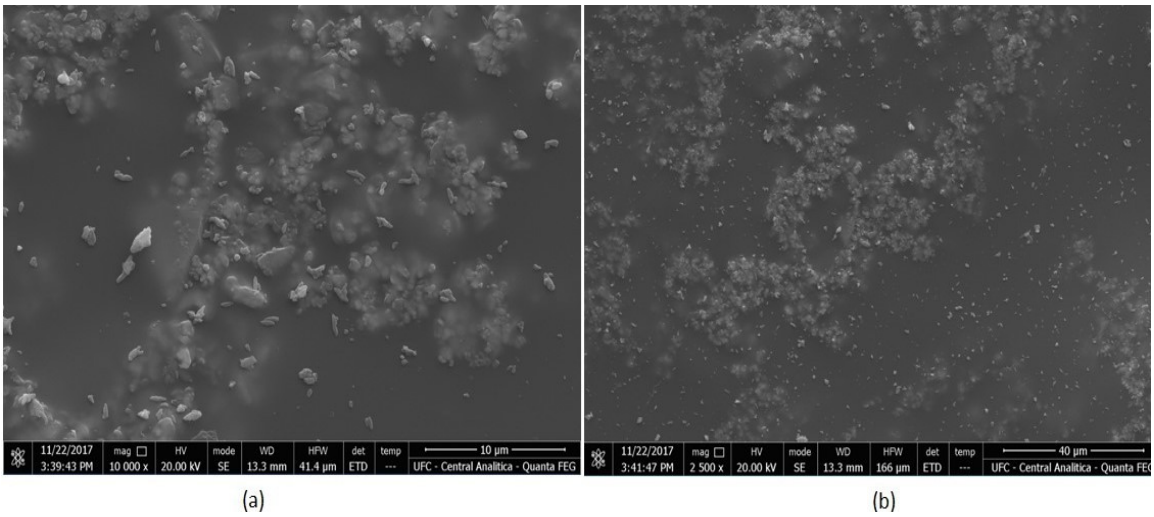


**Figure 6:** Micrograph of the selective surface sample of 50% chromium oxide - 50% granite powder, with magnification factor of: (a) 10000x and (b) 2500x.

In the reference surface (**MR**TiNOX), it can be seen from Figure 7 that almost all of the copper substrate was filled. It is also possible to note a preferential direction of application of the selective surface, as a function of diagonal lines present in practically all the material. With greater approximation, dispersed grains of the main matrix are visualized, being identified oxygen, nickel, aluminum and chrome.

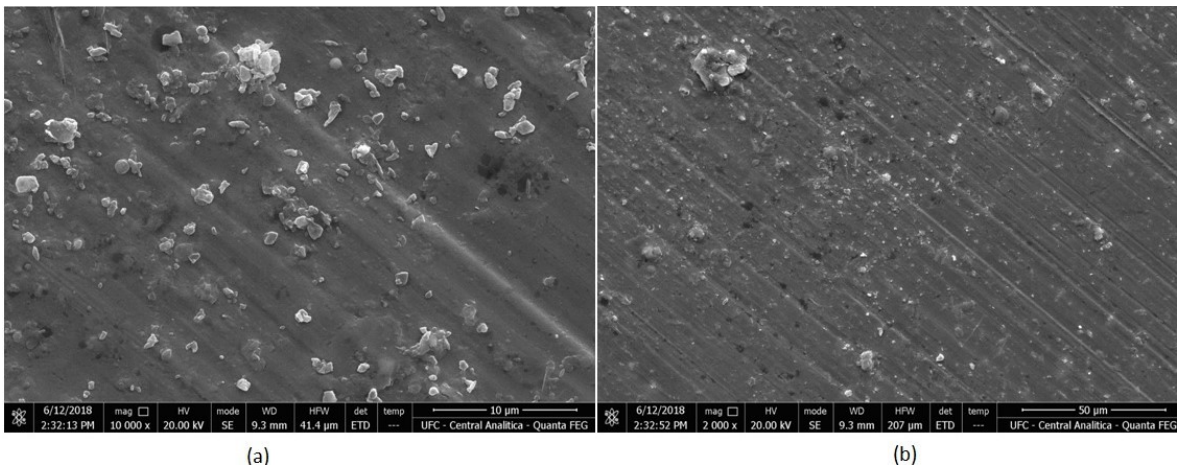


**Figure 7** Micrograph of the **MR**TiNOX selective surface sample, with magnification factor of: (a) 10000x and (b) 2000x.

From the selective surfaces produced, the one that most approached visually of the commercial was 100% granite, according to Figure 8. Although the screen printing technique was also used for all materials, only the granite not mixed with chrome was capable of filling the copper plate in a compact way. As in Figure 7, lines indicating a preferred direction of surface application are present, although with a smaller slope relative to the vertical direction.

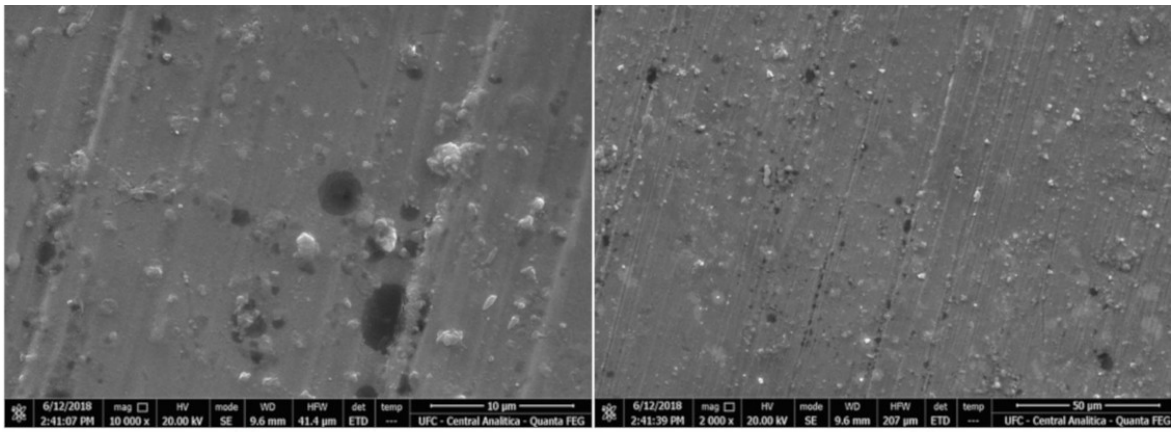


**Figure 8:** Micrograph of the 100% granite selective surface sample, with magnification factor of: (a) 10000x and (b) 2000x.

### 3.4 Structural characterization by XRD

The X-ray diffraction measurement was performed at the X-ray Laboratory of the Physics Department of the UFC. The equipment used was the diffractometer for polycrystalline samples, DMAXB model - Rigaku, X-ray generator of 2KW, with Cobalt (Cu) tube radiation, CuKα1 and CuKα2, operating at 40kV and at 30mA. The identification of the crystalline phases present occurred through the use of the *International Center for Diffraction Data* (ICDD) catalog and the *X'Pert High Score Plus* program. The refinement program used was the GSAS.

In Figure 9, the comparative graph is presented, for the sample of 50% granite powder - 50% chrome oxide, between the pattern observed and the standard calculated during the refinement, yet containing the difference between them.

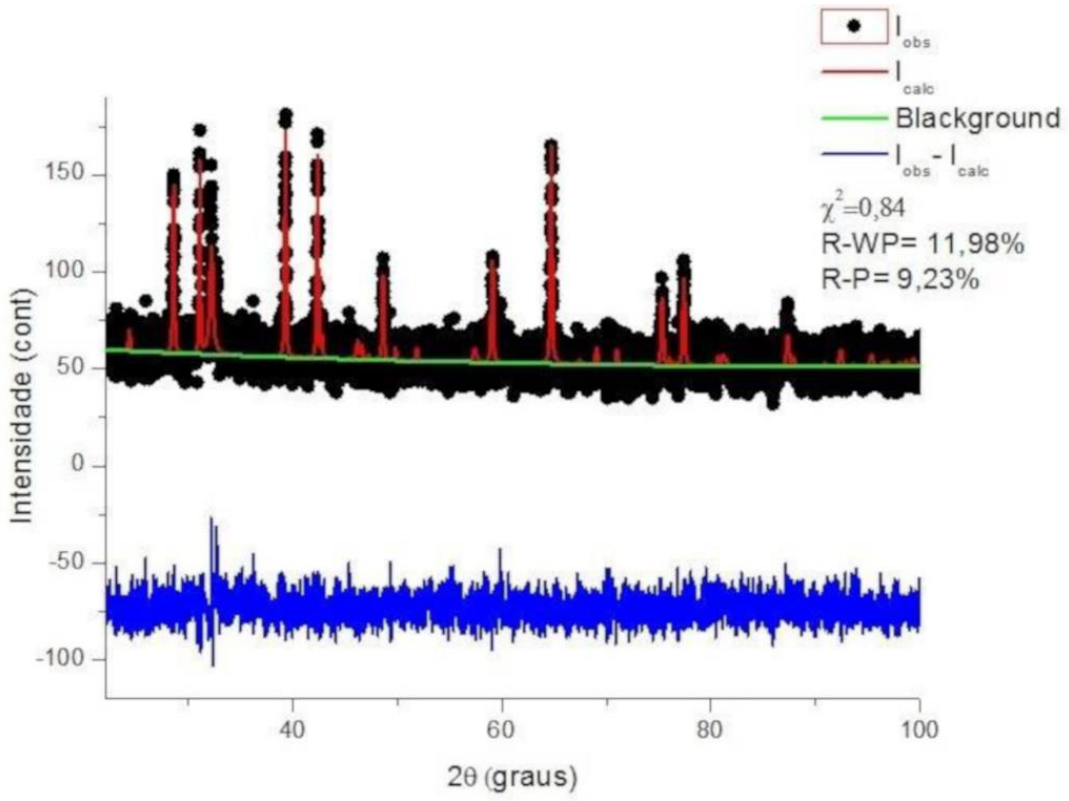


**Figure 9:** Sample diffractogram with 50% granite powder + 50% chrome oxide.

As the refinement cycles were performed, the values of $\chi^2$, R-P and R-WP were decreasing, which consisted of an important indication of the quality of the procedure. The $\chi$ parameter, according to the Rietveld method, should be minimized, obtaining satisfactory results for values close to 1 (one). Also according to the same method, the reliability factors R-P and R-WP are acceptable as nearer 10%.

The phases found for the sample with granite and chrome were: calcium (Ca), chromium oxide ($Cr_2O_3$) and tetrasilicon dioxide ($Si_4O_2$). Considering the reliability factors and the $\chi$ parameter set out in Figure 9, there is a plausible result.

### 3.5 Infrared Analysis

The first spectrophotometers to emerge were the dispersive, of the analog type, being used to obtain the spectrum with monochromatic light. Its main characteristics are: low sensitivity and scanning time of approximately fifteen minutes per sample [15] and [16].

With the development of the microcomputers, it was made use of the instruments of obtaining the IV spectra with Fourier transform. With this, it was possible to perform the spectrum scanning faster when compared to the dispersive spectrophotometer. Another advantage of this evolution is to work with a more precise and reproducible wave number scale [16] and [17].

The absorption spectrum is reached as the continuous spectrum of light passes through a substance. Atoms and molecules generally absorb electromagnetic radiation at the same frequencies as they emit them, so it is said that both emission and absorption spectra are equivalent. This is due to the fact that, in the absorption, there is the inverse transition from the one observed in the emission spectrum [18].

The objective of this characterization was to identify the appearance of some component after the heating of the selective surfaces in a resistive kiln. Thus, analysis for only chrome oxide analysis, for only the granite powder and for the selective surface produced with 50% chrome - 50% granite was performed. The generated graph is shown in Figure 10.

Four major peaks are observed in Figure 10, in the following frequency regions: 4000 to 3500 $cm^{-1}$, 35000 to 3000 $cm^{-1}$, 3000 to 2500 $cm^{-1}$ and approximately 1000 $cm^{-1}$. In all of them, the shape of the peaks coincides, differing only by the intensity, and no new components are obtained after the heating process.

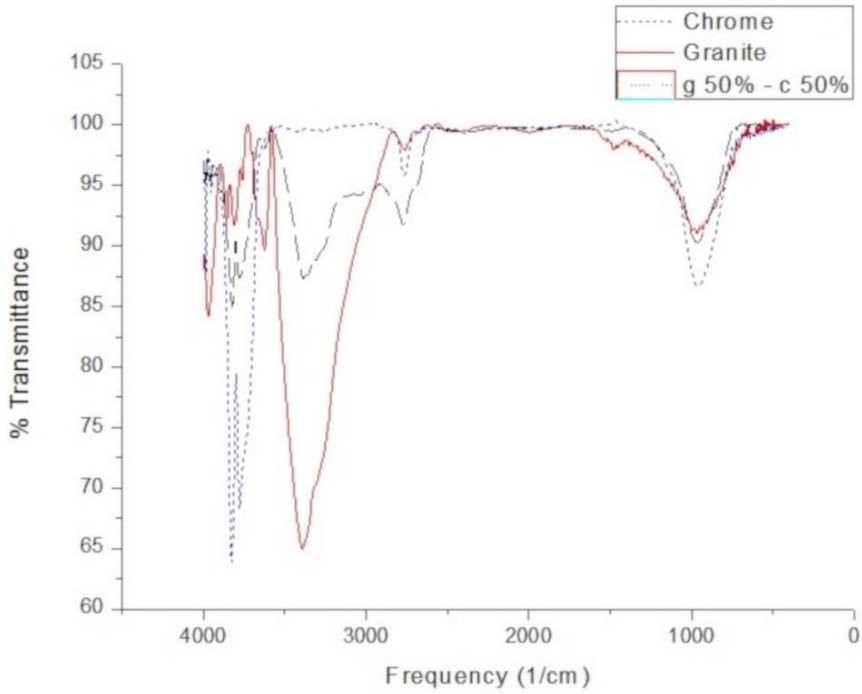


**Figure 10:** Sample transmittance graph with 50% granite powder + 50% chrome oxide.

## 4. DISCUSSION

In order to compare the efficiency of the selective surfaces, it is necessary to perform an energy balance in the test bench with sun exposure. For this, the control volume around the copper substrate will be taken into

account, as shown in Figure 11.

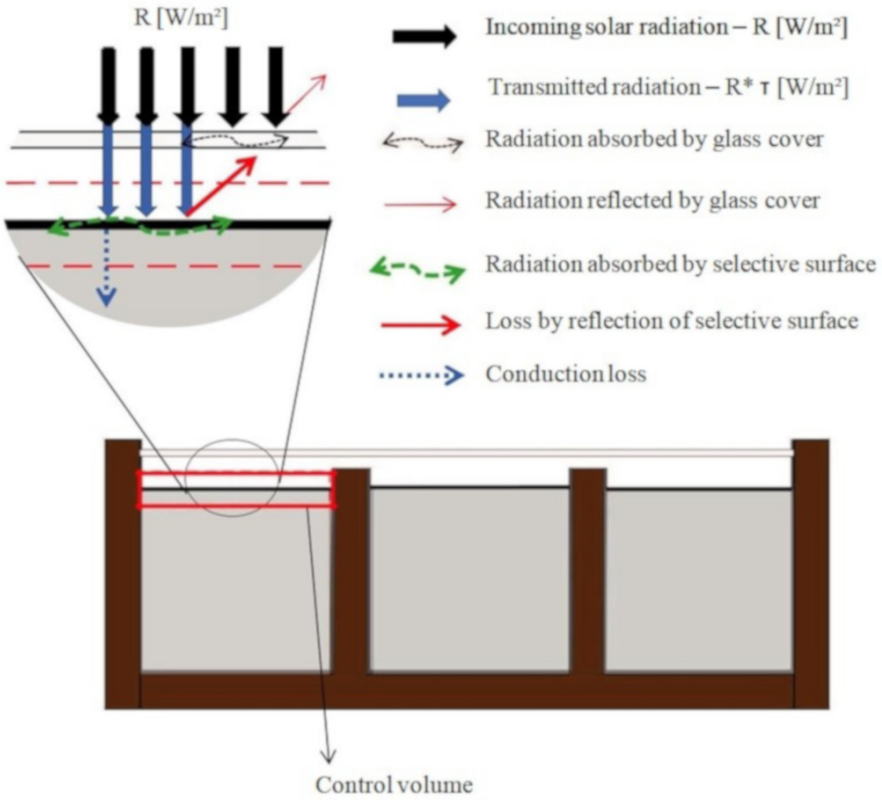


**Figure 11:** Test bench energy balance [7].

The incoming energy (Qin) is related to the solar radiation Rsol (W / m²), with the transmissivity of the glass $\tau_V$ and with the absorptivity $\alpha_S$ and the area of the plate Ap (m²) of the selective surface. Equation 1 represents the energy that arrives at the selective surfaces.

$$Qin = Rsol \times \tau_V \times \alpha_S \times Ap \quad (1)$$

The losses involve the heat exchanged by convection, by conduction, by radiation and by reflection. Due to the glass protection, only the natural convection between the selective surface and the glass cover is considered. The conduction loss occurs by thermal insulation, which has a thickness L of 5cm and thermal conductivity K of 0.04 W / mK. The Stefan-Boltzmann constant ($\sigma$ = 5,67 x 10-8 W/m²K$^4$) is used for radiation-related energy calculations. The energy lost by reflection represents the solar radiation reflected by the surface of the copper plates. Each of these parts is represented in equations 2 to 5.

$$Qconv = h \times Ap \times (Tp - Tcg) \quad (2)$$

$$Qcond = \frac{K}{L} \times Ap \times (Tp - Tb) \quad (3)$$

$$Qrad = \varepsilon \times Ap \times \sigma \times (Tp^4 - Tcv^4) \quad (4)$$

$$Qref = (1 - \alpha_S) \times Rsol \times Ap \quad (5)$$

Where: Tp is the plate temperature; Tcg is the temperature of the glass cover; h is the coefficient of heat transmission by convection; Tb is the temperature near the outer wall of the structure; $\varepsilon$ is the emissivity of the selective surface.

For the control volume of Figure 11, the energy balance is indicated in equation 6. The transformed heat rate is zero because no power generation occurs.

$$Qaccumulated = Qin - Qout + Qtransformed \quad (6)$$

In steady state, with the temperatures stabilization, the accumulated energy rate becomes zero. Thus, by inserting equations 1 to 5 in equation 6, the energy balance can be expressed by:

$$Rsol \times \tau_V \times \alpha_S \times Ap = \varepsilon \times Ap \times \sigma \times (Tp^4 - Tcg^4) + h \times Ap \times (Tp - Tcv) + \frac{K}{L} \times Ap \times (Tp - Tb) + (1 - \alpha_S) \times Rsol \times Ap \quad (7)$$

As the selective surfaces produced are not commercially available, their absorptivity and emissivity properties are not known, and it is needed to be calculated by equation 7. To do so, it is used equation 8, which represents the useful energy supplied by a solar collector to the fluid of work [19].

$$Quseful = Ap\,[Rsol \times \tau_V \times \alpha_S - Ul\,(Tp - Ta)] \quad (8)$$

The overall coefficient of heat loss (Ul) is the same for all surfaces, since the operating conditions were identical. For the situation in question, since there is no use of thermal fluid, Quseful = 0. Thus, equation 9 is obtained, which is the adaptation of equation 8 for this study, considering Ta the ambient temperature.

$$Ul = Rsol \times \tau_V \times \alpha_S / (Tp - Ta) \quad (9)$$

The commercial selective surface (**MR**TiNOX) has absorbance $\alpha_S$ = 0.95 and emissivity ε = 0.04, according to the manufacturer's data [20]. The transmissivity of the glass used is 0.87. Considering that the average radiation, for the interval from 11h to 12:30h, according to the graph of Figure 3, was 938.4 W / m², and that the commercial plate and ambient temperatures were 92.7 °C and 34.0 °C, respectively, according to Table 2, the calculated global heat loss coefficient was Ul = 13.21.

Applying equation 7 to the commercial surface, knowing that the area of the plate used was Ap = 8 x $10^{-4}$ m², a coefficient of convection heat transfer h = 27.07 W / m²K was found. Based on a range of 5 to 30 W / m²K for this coefficient, in natural convection applications [21], the result calculated is assumed as plausible.

For the selective surfaces produced, using the result for calculated Ul, the absorbance values are obtained by equation 9. Then, by equation 7, the emissivity of each surface is found. In order to compare the efficiency (f) of all selective surfaces, the absorptivity is divided by emissivity. For values f > 18, the absorber surface is considered highly selective [20]. All data obtained are summarized in Table 3.

**Table 3:** Emissivity and absorptivity of selective surfaces.

| SURFACE | ABSORPTIVITY | EMISSIVITY | EFFICIENCY |
|---|---|---|---|
| Surface 100% granite | 0,86 | 0,038 | 22,61 |
| Surface granite 75% - chrome 25% | 0,84 | 0,037 | 22,60 |
| Surface granite 50% - chrome 50% | 0,86 | 0,038 | 22,61 |
| Surface granite 25% - chrome 75% | 0,88 | 0,039 | 22,69 |
| Surface 100% chrome | 0,91 | 0,040 | 22,95 |
| **MR**TiNOX | 0,95 | 0,040 | 23,37 |

Although no selective surface produced has exceeded the efficiency value of the commercial product, the emissivities found of those were equal to or less than the emissivity of this, and all of them can be considered highly selective.

## 5. CONCLUSIONS

Although none of the selective surfaces produced have exceeded the efficiency of the trademark **MR**TiNOX, they can all be considered highly selective, which represents a major step towards reducing the cost of solar collectors. The surface produced only with chromium oxide was the one that presented the closest efficiency to the commercial, but those with granite powder reached satisfactory values for use in works with solar energy.

The main difference between the analyzed surfaces occurred in the absorptivity, varying from 0.84 to 0.95. The values of emissivity found were very close, and some selective surfaces produced reached numbers even smaller than the commercial product.

One of the ways to try to obtain better values for the efficiencies is to change the technique of applying the selective surfaces on the copper substrate. The process used in this work was the *screen printing*, but other forms of deposition, such as *spin coating*, could be tested.

## 6. ACKNOWLEDGMENTS

This work would not be possible without the support of some people who enabled the preparation and characterization of the selective surfaces, thanking:

1. Prof. Dr. Sérgio Sombra, for having authorized the use of the planetary mill in order to obtain the granite powder, besides providing boron oxide and bismuth oxide to prepare the flux, and to the member of the Laboratory of Telecommunications and Science and Engineering of Materials (LOCEM), João Paulo, for conducting the grinding process;

2. The laboratory technique Nadia Aline de Oliveira Pitombeira, for conducting the infrared analysis and the absorbance tests, in the Chemistry Department of the UFC;

3. The Central Analytical of the UFC, by the characterization by MEV;

4. The members of the UFC X-ray Diffraction Laboratory, for authorizing the X-ray diffraction analysis of the selective surface produced;

5. The teachers Paulo Alexandre and Maria Eugênia, from the Laboratory of Solar Energy and Natural Gas, for yielding a space for the tests in the sun, as well as for providing the data of solar radiation in the days of the field tests.

## 7. BIBLIOGRAPHY

[1] RAMOS, R.E.B., *Análise de desempenho de um fogão solar construído a partir de sucatas de antena de TV*, Dissertation of M.Sc., UFRN, Natal, 2011.

[2] EPE - EMPRESA DE PESQUISA ENERGÉTICA, Balanço Energético Nacional 2017 – Ano base 2016: Relatório Síntese, Rio de Janeiro, 2017.

[3] LION, C. A. P. Q., *Construção e análise de desempenho de um fogão solar à concentração utilizando dois focos para cozimento direto*, Dissertation of M.Sc., UFRN, Natal, 2007.

[4] QUASCHNING, V., *Understanding Renewable Energy Systems*, 3 ed, London, Earthscan, 2005.

[5] GRANQVIST, C.G., "Solar-energy materials - overview and some examples", Applied Physics A, v. 52, n. 2, pp. 83-93, Feb. 1991.

[6] TEIXEIRA, V., *et al*., "Spectrally selective composite coatings of Cr-Cr2O3 and Mo- Al2O3 for solar energy applications", Thin Solid Films, v. 392, pp. 320-326, July 2001.

[7] KATZEN, D., LEVY, E., *et al*., "Thin Films of Silica-Carbon Nanocomposites For Selective Solar Absorbers", Applied Surface Science, v. 248, pp. 514-517, July 2005.

[8] BARSHILIA, H. C., SELVAKUMAR, N., *et al*., "Thermal stability of TiAlN/TiAlON/Si3N4 tandem absorbers prepared by reactive direct current magnetron sputtering", *Journal of Vacuum Science and Technology A*, v. 25, n. 2, p. 383, Jan. 2007.

[9] ESTUDO EQUINÓCIO SOLARENERGY, *Energia Solar em Habitações do Programa Minha Casa Minha Vida*, Curitiba, 2011.

[10] SELVAKUMAR, N., *et al*., "Spectrally selective CrMoN/CrON tandem absorber for mid-temperature solar thermal applications", *Solar Energy Materials & Solar Cells*, v. 109., pp. 97-103, Feb. 2013.

[11] PEREIRA. E. B., MARTINS. F. R., *et al*., *Atlas brasileiro de energia solar*, 2 ed., São José dos Campos, INPE, 2017.

[12] VIEIRA, S. G., *Obtenção, caracterização e aplicação de uma nova superfície seletiva para coletores solares térmicos*, Dissertation of M.Sc., UFC, Fortaleza, 2011.

[13] RODRIGUES, F.P., *Obtenção e estudo de uma superfície seletiva para coletores solares térmicos a partir de resíduos de granito*, Dissertation of M.Sc., UFC, Fortaleza, 2014.

[14] GALLETI , S. R., "Introdução à Microscopia Eletrônica", *Instituto Biológico*, v. 65, n. 1/2, pp.33-35, Jan./Dez. 2003.

[15] BRAGANÇA, S. R., BERGMANN, C. P., "Microestrutura e propriedades de porcelanas", *Cerâmica [online]*, v. 50, n. 316, pp. 291-299, Out./Dez. 2004.

[16] GRIFFTHS, P. R., *Chemical Infrared Fourier Transform Spectroscopy*, 1 ed., New York, John Wiley & Sons, 1975.

[17] BRAIMAN, M. S., ROTHSCHILD, K. J., "Fourier Transform Techniques for Probing Membrane Protein Structure", *Ann. Rev. Biophys. Chem*., v. 17, pp. 541-570, June 1988.

[18] GRIFFTHS, P. R., SLOANE, H. J., *et al*., "Interferometers vs Monochromators: Separating the Optical and Digital Advantages", Appl. Spectrosc., *Baltimore*, v. 31, n. 6, pp. 485-495, Nov. 1977.

[19] LEITE, D. O., PRADO, R. J., "Espectroscopia no infravermelho: uma apresentação para o Ensino Médio", *Rev. Bras. Ensino Fís. [online]*, v. 34, n. 2,pp. 1-9, Jun. 2012.

[20] KALOGIROU, S. A., "Prediction of flat-plate collector performance parameters using artificial neutral networks", *Solar Energy*, v. 80, n. 3, pp. 248-259, Mar. 2006.

[21] ALMECO GROUP, http://www.almecogroup.com/uploads/1172-ALMECO_TinoxEnergy_ENG_S402_07_2014_mail.pdf. Accessed in August 2018.

[22] UNESP, http://www.dem.feis.unesp.br/intranet/tci_capitulo1.pdf. Accessed in August 2018.

[23] SASI, A. S, *Energy efficiency of solar heat concentrators using glass coated Al doped ZnO transparent conducting oxide as selective absorber*, Tese of D.Sc, Cape Peninsula University of Technology, Cape Peninsula, 2017.

[24] NUNES, R. A. X., *et al*., "Selective Surfaces of Black Chromium for Use in Solar Absorbers", *Mat. Res. [online]*, v. 21, n. 1, Nov. 2017.

## ORCID

Felipe Alves Albuquerque Araújo https://orcid.org/0000-0002-6392-7853
Francisco Nivaldo Aguiar Freire https://orcid.org/0000-0001-5195-1402
Diego Caitano Pinho https://orcid.org/0000-0001-9324-3375
Kaio Hemerson Dutra Sem ORCID
Paulo Alexandre Costa Rocha https://orcid.org/0000-0002-4366-366X
Maria Eugênia Vieira da Silva https://orcid.org/0000-0002-3177-3052